Real-Time Vibronic Coupling Dynamics in a Prototypical Conjugated Oligomer

G. Cerullo,[1,2] G. Lanzani,[1,3] M. Muccini,[4] C. Taliani,[4] and S. De Silvestri[1,2]

[1]*Istituto Nazionale per la Fisica della Materia, Italy*
[2]*CEQSE C.N.R., Dipartimento di Fisica, Politecnico di Milano, 20133 Milano, Italy*
[3]*Istituto di Matematica e Fisica, Universita' di Sassari, 07100 Sassari, Italy*
[4]*Istituto di Spettroscopia Molecolare del C.N.R., 40129 Bologna, Italy*

(Received 5 November 1998)

Phonon modes which are strongly coupled to the lowest optical transition of α-sexithienyl are directly probed in real time by coherent vibrational spectroscopy. The resonant excitation source is a tunable 10-fs optical parametric amplifier. We identify five strongly coupled phonon modes at $\omega_1 = 112$ cm^{-1}, $\omega_2 = 299$ cm^{-1}, $\omega_3 = 702$ cm^{-1}, $\omega_4 = 1040$ cm^{-1}, and $\omega_5 = 1454$ cm^{-1}. Vibrational dephasing times are measured to be between 0.4 and 3 ps. We gain direct hints on potential energy anharmonicity by measuring the transient vibrational frequency within the first ps.

PACS numbers: 78.47.+p, 78.55.Kz, 78.66.Qn

Conjugated polymers and oligomers are a new and promising class of organic semiconductors with applications in electronics and optoelectronics; in particular, prototypes of light emitting diodes, lasers, and photovoltaic cells were recently demonstrated [1]. These advances have been constantly backed by a fundamental research effort aimed at clarifying the excitation processes in these systems: a deeper understanding of their photophysics helps to engineer better materials and to improve device performance.

In linear conjugated chains the π electrons are strongly coupled to a few normal modes of the carbon backbone, having the right symmetry to induce dimerization. This coupling induces a gap in the electronic density of states that is modulated by total-symmetric vibrations of the dimerization amplitude, the so-called "amplitude modes" [2,3]. These are Raman active modes which appear in the vibronic structure of the optical transition too [4]. The direct observation of the amplitude modes in conjugated polymers is highly relevant for the understanding of the excited state relaxation and of their linear and nonlinear optical properties. Thiophene oligomers and α-sexithienyl (α-T_6), in particular, are among the most well studied model compounds for understanding the photophysics of conjugated polymers [5]. In addition, α-T_6 has been used to build field-effect transistors with characteristics suitable for large-scale low cost applications [6]. Its electronic structure has been extensively studied by quantum-chemical calculation [7,8] and by optical and vibrational spectroscopy [9,10]. The involvement of the Herzberg-Teller mechanism in the vibronic coupling, as well as the relaxation of the modes in the excited state, has been pointed out [11,12]. In general, the vibronic spectra obtained with traditional techniques are quite complex, and their assignment presents ambiguities due to the dramatic influence of broadening effects and to the presence of traps and molecular defects.

The development of femtosecond laser sources has allowed one to probe coherent nuclear motion in real time. Collective vibrational coherence among oscillating molecules can be induced if the laser pulse is sufficiently short compared with the characteristic period of the mode [13]. In resonant experiments this technique, known as impulsive coherent vibrational spectroscopy (ICVS), provides unique spectral and dynamic information on the optically coupled phonon modes. However, direct time domain investigation of the vibronic structure in conjugated polymers has been limited to date [14] by the lack of a reliable source of tunable sub-20-fs pulses in the visible region of the spectrum.

In this paper we apply for the first time the ICVS technique to study the vibrational dynamics in π-conjugated chains. Our results demonstrate the general validity of ICVS as a tool for studying vibronic coupling dynamics in the time domain. This advance is made possible by the recent availability of a new laser source [15] which allows one to probe with extremely high time resolution systems absorbing in the blue-green spectral range. We choose the model molecule of α-sexithienyl (α-T_6) in the form of polycrystalline thin films. Coherent oscillations with frequencies up to 1500 cm^{-1} are observed in the time domain. This result allows one to identify all the total symmetric (a_g) modes which are coupled to the electronic transition and removes the uncertainties of the previous interpretation based on conventional optical spectroscopy [11,12], leading to a conclusive assignment of the vibronic structure in α-T_6. In addition, these data provide a wealth of new information on the vibronic dynamics [16], such as direct measurement of vibrational damping and mode anharmonicity.

The experiments were performed using a novel optical parametric amplifier (OPA) based on noncollinear phase matching in β-barium borate [15]. The OPA provides pulses with bandwidths broader than 50 THz, 10–12 fs duration, and center wavelengths tunable from 490 to 700 nm. The measurements are performed with a noncollinear pump-probe setup; after the sample the probe beam, selected by an iris, is detected by a photodiode

followed by a lock-in amplifier. Single wavelengths of the broadband probe pulse are selected using 10 nm bandwidth interference filters after the sample. Polycrystalline α-T_6 films with an approximate thickness of 100 nm, vacuum deposited at standard conditions [17], are excited by 10–12 fs pulses with central wavelength of 510 nm, close to the first absorption peak. The experiments are performed at room temperature and in the linear excitation regime.

Figure 1 shows the differential transmission (ΔT) of the α-T_6 film vs pump-probe delay at the probe wavelength of 510 nm. The features at negative and near-zero delays at this and other wavelengths are due to pump-perturbed free induction decay and coherent coupling [18]. For positive delays we observe a negative ΔT signal, growing in approximately 200 fs. Since the primary photoexcitations in solid α-T_6 are tightly bound Frenkel excitons [19], we attribute the signal to superposition of ground-state bleaching and photoinduced absorption (PA) originating from the exciton level. This initial competition cannot be due to coherent artifacts because it takes place at time delays exceeding the pulse duration. We assign this behavior to exciton intraband relaxation populating lower lying states, from which absorption takes place. The PA signal is modulated by a complex oscillatory pattern, caused by the motion of the wave packet launched by the pump pulse on the multidimensional excited state potential energy surface (PES). The inset of Fig. 1 shows the Fourier transform of the oscillatory component of the signal, after subtracting a slowly varying background. We clearly identify five modes, at frequencies $\omega_1 = 112$ cm^{-1}, $\omega_2 = 299$ cm^{-1}, $\omega_3 = 702$ cm^{-1}, $\omega_4 = 1040$ cm^{-1}, and $\omega_5 = 1454$ cm^{-1}, respectively.

Measurements at other wavelengths show either bleaching or PA; in all cases the signal is modulated by an oscillatory pattern due to the same five characteristic frequencies. Figure 2 shows, for instance, ΔT at 540 nm, close to the absorption edge in the T_6 film. The relative intensities of the frequencies depend on the probing wavelength (see inset of Fig. 2). The reason for this difference is that, changing the probe wavelength, we probe different regions of the multidimensional excited state PES [16,20]. Because of the low ground-state absorption cross section at 540 nm, we assign the rapidly decaying positive signal at early times to stimulated emission from the excited state, which is then masked by the PA growth.

In both Figs. 1 and 2 it is shown that the oscillations persist almost undamped for delays longer than 1 ps. To measure the characteristic coherence time decay we extended the experiment time scale out to 8 ps with an interval between sampling points of 25 fs. Since this time step is insufficient to correctly sample the higher frequency oscillations, on this time scale the signal is dominated by the lowest frequency mode at ω_1, as shown in Fig. 3. A fit with an exponentially damped sinusoid gives a damping time of 3 ps, corresponding to a linewidth of 3 cm^{-1}. Note that the measured dephasing time of ω_1 is considerably longer than that generally assumed for vibrational energy redistribution, which is of the same order of magnitude of the vibrational period. This finding provides new insight into the early processes of excess energy redistribution in excited molecules: In contrast with the conventional pictures, we obtain evidence that the initial relaxation, occurring in approximately 200 fs, does not lead to a full thermalization but to an intermediate state dissipating the energy stored in low-frequency vibrations on a much longer time scale.

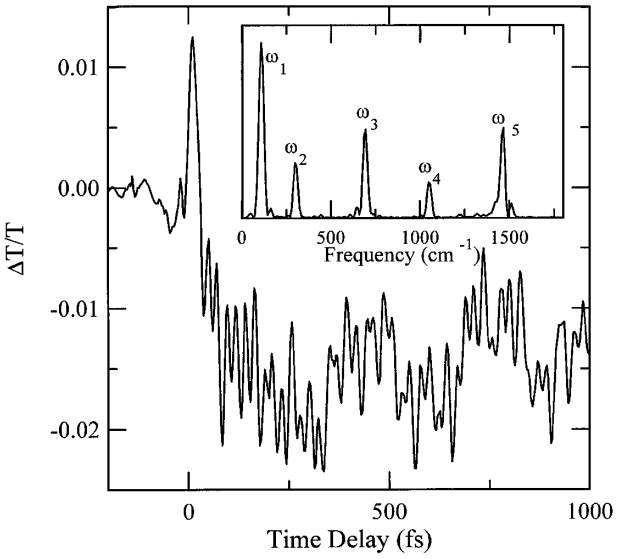

FIG. 1. Differential transmission dynamics $\Delta T/T$ for the α-T_6 film at 510 nm probe wavelength. The inset shows the Fourier transform of the oscillatory component of the signal.

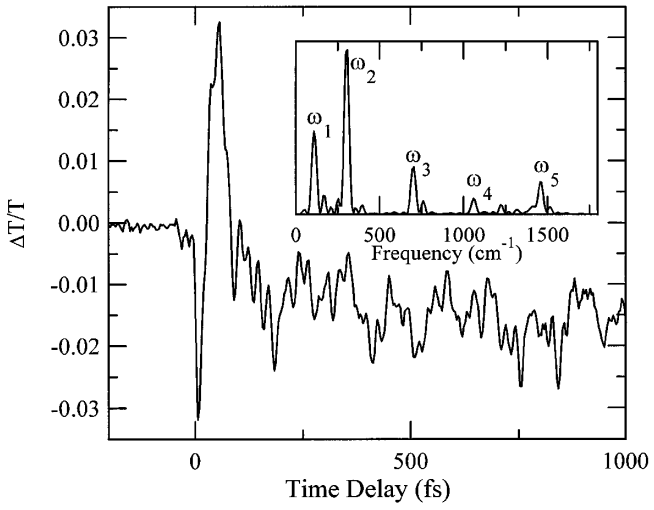

FIG. 2. Differential transmission dynamics $\Delta T/T$ for the α-T_6 film at 540 nm probe wavelength. The inset shows the Fourier transform of the oscillatory component of the signal.

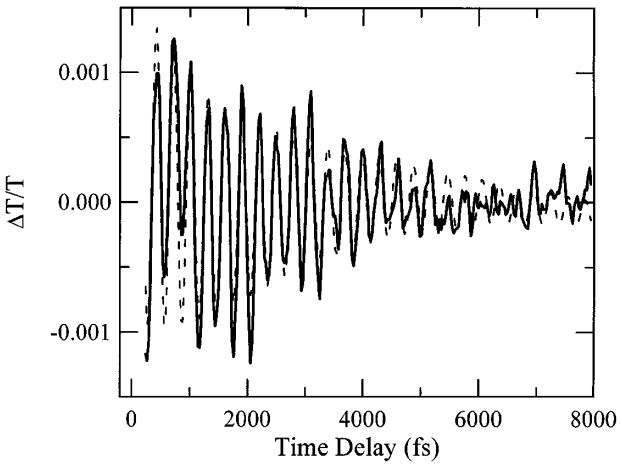

FIG. 3. Oscillatory component of the signal at 510 nm (solid line) for pump-probe delays up to 8 ps and fit with an exponentially damped sinusoid (dashed line).

Let us now discuss the assignment of the observed vibrational modes. Recently, low temperature polarized absorption and photoluminescence of single crystals allowed the tentative assignment of the total-symmetric modes coupled to the lowest singlet $1B_u$-$1A_g$ transition [11,12]. The lowest energy modes at $\omega_1 = 112$ cm^{-1} and $\omega_2 = 299$ cm^{-1} correspond to the 126 cm^{-1} and 297 cm^{-1} ones proposed to interpret the absorption of the single crystal [12]. In this view ω_1 and ω_2 are Herzberg-Teller active modes which couple the two lowest singlet excited states of the molecule (1^1B_u and 2^1B_u) and give rise to the polarized false origins at 18 486 cm^{-1} (O′) and 18 657 cm^{-1} (O″), respectively. These vibronic levels lie above the electronic origin of the absorption and are shifted in energy by $\hbar\omega_1$ and $\hbar\omega_2$. However, the ICVS signal at ω_1 and ω_2 is due to coherent motion in the excited PES of vibrational wave packets built on the corresponding Franck-Condon manifold. We can exclude quantum beats between O′ and O″ due to their different polarization and very weak oscillator strength. ICVS supports their definitive assignment to total symmetric (a_g) intramolecular modes [11,12].

The frequencies $\omega_3 = 702$ cm^{-1}, $\omega_4 = 1040$ cm^{-1}, and $\omega_5 = 1454$ cm^{-1} closely correspond to the ground-state modes measured by fluorescence and Raman spectroscopy in α-T_6 single crystal [11] at 699, 1056, and 1460 cm^{-1}, respectively. We thus assign these modes to carbon-carbon bending and stretching [8]. Table I summarizes the comparison of the vibrational modes determined by ICVS with those obtained by *ab initio* calculation and high-resolution conventional spectroscopic techniques. ICVS has some distinct advantages with respect to the latter, which require highly ordered samples at very low temperatures and result in complicated vibronic structures. In contrast, ICVS can be applied to disordered materials at room temperature, due to the selective detection of pure total-symmetric modes coupled to the electronic transition. In addition, for highly luminescent materials, it is a valid alternative to other time-resolved vibrational spectroscopies.

The decay of the amplitude of the observed oscillations, reported in Table I, is directly related to the molecular vibrational dephasing times. The higher frequency modes have faster dephasing, as observed for ω_5 with $\tau_5 =$ 0.4 ps. We speculate that this is due to excited state energy relaxation redistributing the energy. For high-frequency modes, having only a few components in the wave packet, this corresponds to a total coherence loss. In this experiment we measure the dephasing time of the vibrational polarization, and not the dephasing time of the polarization of the vibronic transition, which is much shorter.

To determine the PES characteristics, the Fourier transforms of the oscillatory components of the signal at 510 nm performed on two separate time windows, 0–500 and 500–1000 fs, are shown in Fig. 4. We observe a clear shift of the ω_5 mode towards higher frequency for

TABLE I. Comparison of the a_g vibrational modes obtained by ICVS in a polycrystalline α-T_6 thin film and by conventional spectroscopy in a single crystal. The totally symmetric vibrations of the ground state measured in the Raman spectrum excited in preresonance conditions [21] and in the fluorescence spectrum [11] are compared with the results of *ab initio* calculation [8]. The corresponding vibrations in the excited state are measured in the absorption spectrum [12]. The damping times of the oscillatory signal are obtained using a single-value decomposition algorithm.

Ground state			Excited state	ICVS		Assignment
Raman (cm^{-1})	Photoluminescence (cm^{-1})	Calculation (cm^{-1})	Absorption (cm^{-1})	(cm^{-1})	Damping times (ps)	
169	165	147	126	112	3	a_g(41), SCC bending
306	306	305.5	297	299	2	a_g(39), CSC bending
699	699	702	660	702	0.9	a_g(33), CSC bending
1056	1056	1061.8		1040	0.7	a_g(25), CβCβ stretching, CCH bending
1460	1460	1459.6	1275	1454	0.4	a_g(11), CαCα, CβCβ stretching

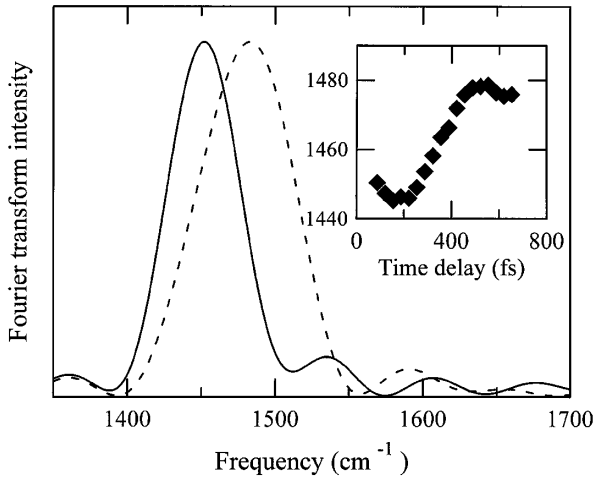

FIG. 4. Fourier transforms of the oscillatory component of the signal in Fig. 1 for the time windows 0–500 fs (solid line) and 500–1000 fs (dashed line); the inset shows the peak frequency of 300 fs blocks of the signal as a function of delay.

increasing time delays. This time evolution is better depicted in the inset of Fig. 4 showing the peak of the Fourier transform of 300 fs blocks of the signal, each shifted by 50 fs, as a function of time delay. To understand this result, we recall that the period of the ω_5 mode is short enough to cause sizable displacement of the polarization wave packet on the excited PES during pump excitation. It is thus possible, by a second interaction with the pump field, to bring the wave packet down to the ground state, well out of the equilibrium position corresponding to the PES minimum. We thus generate a vibrational wave packet within the ground state PES: In the presence of anharmonicity its relaxation is associated with a change in the vibrational frequency, as indeed observed by ICVS. Oscillating closer to the PES minimum, the wave packet samples the most harmonic part of the well, and correspondingly we measure a higher oscillation frequency. By assigning the frequency shift to this process we obtain an estimate for the excess relaxation time in the ground state of about 300 fs, of the same time scale as ω_5 dephasing.

In conclusion, we have applied the ICVS technique to the detection of total-symmetric vibrational modes in α-T_6 polycrystalline films. Five modes strongly coupled to the π-π^* electronic transition are identified, with frequencies up to $\approx$1500 cm^{-1}. These data, together with those obtained with conventional techniques in the single crystal at low temperature, allow one to unambiguously determine the vibronic structure of α-T_6. In addition, damping times of the vibrational coherence and PES anharmonicity are measured. These results open up new possibilities for characterizing vibronic transitions in a wide class of π conjugated materials, which cannot be obtained in the form of single crystals as required for conventional high-frequency resolution spectroscopy.

[1] R. H. Friend *et al.*, Nature (London) **397**, 121 (1999).
[2] E. Ehrenfreund, Z. Vardeny, O. Brafman, and B. Horovitz, Phys. Rev. B **36**, 1535 (1987).
[3] G. Zerbi, B. Chierichetti, and O. Ingänas, J. Chem. Phys. **94**, 4637 (1991).
[4] F. Negri and Z. Zgierski, J. Chem. Phys. **100**, 2571 (1993).
[5] C. Taliani and L. M. Blinov, Adv. Mater. **8**, 353 (1996).
[6] A. Dodabalapur, L. Torsi, and H. E. Katz, Science **268**, 270 (1995).
[7] D. Beljonne *et al.*, J. Chem. Phys. **118**, 6453 (1996).
[8] A. Degli Esposti *et al.*, J. Chem. Phys. **104**, 9704 (1996).
[9] R. S. Becker, J. Seixas de Melo, A. L. Macanita, and F. Elisei, J. Phys. Chem. **100**, 18 683 (1996); D. Birnbaum, D. Fichou, and B. E. Kohler, J. Chem. Phys. **96**, 165 (1992).
[10] G. Louarn, J. P. Buisson, S. Lefrant, and D. Fichou, J. Phys. Chem. **99**, 11 399 (1995).
[11] M. Muccini *et al.*, J. Chem. Phys. **108**, 7327 (1998).
[12] M. Muccini *et al.*, J. Chem. Phys. **109**, 10 513 (1998).
[13] H. L. Fragnito, J.-Y. Bigot, P. C. Becker, and C. V. Shank, Chem. Phys. Lett. **160**, 101 (1989).
[14] J.-Y. Bigot, T.-A. Pham, and T. Barisien, Chem. Phys. Lett. **259**, 469 (1996).
[15] G. Cerullo, M. Nisoli, and S. De Silvestri, Appl. Phys. Lett. **71**, 3616 (1997); G. Cerullo, M. Nisoli, S. Stagira, and S. De Silvestri, Opt. Lett. **16**, 1283 (1998).
[16] A. E. Johnson and A. B. Myers, J. Chem. Phys. **104**, 2497 (1996).
[17] F. Biscarini *et al.*, Phys. Rev. B **52**, 14 868 (1995).
[18] C. H. Brito Cruz *et al.*, IEEE J. Quantum Electron. **QE-24**, 261 (1988).
[19] G. Lanzani *et al.*, Phys. Rev. Lett. **79**, 3066 (1997).
[20] W. T. Pollard *et al.*, J. Phys. Chem. **96**, 6147 (1992).
[21] G. Ruani *et al.* (to be published).